Jpn. J. Appl. Phys. Vol. 32 (1993) pp. 4542–4549
Part 1, No. 10, October 1993

Photoluminescence Studies in $CuAlS_2$:Zn

Igor AKSENOV, Masahiro MATSUI[1], Tetsuya KAI and Katsuaki SATO*
Faculty of Technology, Tokyo University of Agriculture and Technology, Koganei, Tokyo 184
[1]*Central Laboratory, Asahi Chemical Industry Co. Ltd., Samejima, Fuji 416*

(Received January 22, 1993; accepted for publication August 21, 1993)

Photoluminescence properties of Zn-doped $CuAlS_2$ crystals have been studied in connection with the composition and crystal phases of the samples. It has been found out that Zn at relatively low concentration introduces a deep donor-like defect in the band gap of a host compound, whereas doping with Zn in a high concentration results in a formation of a multiphase structure on the surface and in the presurface region of the samples, this structure resulting in an enhancement of blue and green luminescence inherent to the lightly Zn-doped $CuAlS_2$ phase.

KEYWORDS: $CuAlS_2$ ternary compound, Zn-doping, photoluminescence spectrum, multiphase structure

1. Introduction

$CuAlS_2$ ternary semiconductor is the widest band gap member of $A^1B^3C_2^6$-type compounds which crystallizes in the tetragonal chalcopyrite structure and is expected to be a possible candidate for blue-to-ultraviolet light emitting device application.

The typical photoluminescence (PL) spectrum of undoped $CuAlS_2$ crystals, grown by the chemical vapour transport (CVT) technique, has been found to exhibit several emissions in different spectral regions, that is

(1) a series of sharp lines in the ultraviolet spectral region, 346–357 nm, caused by the recombination of free and bound excitons,[1] the position of the free exciton emission having been found to be at 349.3 nm (3.550 eV) at 10 K,

(2) several weak free-to-bound transitions in the violet spectral region, peaked at 372, 378, and 383 nm (under an electron beam excitation the first two peaks shift to 370 and 374 nm, respectively), presumably related to native defects,[2]

(3) a series of intense emissions in the purple spectral region from 406 to 423 nm, supposedly originated from the donor-acceptor (DA)-pair recombination involving native defects and residual impurities,[1,3] and

(4) a broad orange emission peaked at 590–620 nm, originated from DA-pair recombination involving deep levels.[4]

Although the intensities of the above mentioned emissions vary from sample to sample, in most of the CVT-grown undoped $CuAlS_2$ crystals the orange emission band has been found to dominate both the PL and cathodoluminescence spectra, and, therefore, an orange-coloured emission from the crystals is usually observed under photo- or electron beam-excitation.

Doping of the $CuAlS_2$ crystals with Zn by annealing of the samples in the presence of Zn-metal causes drastic changes in the physical properties of these crystals. The observation of the very efficient blue and green emissions from the Zn-doped crystals, those emissions being bright even at room temperature (RT), has been reported,[5] and low resistivity samples of both p- and n-types of conductivity have been obtained by Zn-doping.[6]

*To whom reprint requests should be addressed.

However, it has been recently found out that

(1) the dominant colour of emission from the Zn-doped samples depends not only on the Zn-doping conditions but also on the distance from the surface of the sample, i.e. a step-by-step polishing of the sample causes the change in the colour of the emission, and

(2) samples annealed in Zn at the same annealing conditions exhibit sporadically either p- or n-type of conductivity.

Above-mentioned strange properties, implying inhomogeneous distribution of Zn in the samples, causes us to investigate the microstructure and morphology of the Zn-doped $CuAlS_2$. In this paper we report the results of the PL studies of the Zn-doped $CuAlS_2$ in connection with the composition and multi-phase structure of samples.

2. Experimental

2.1 *Crystal growth*

Single crystals were grown by the CVT technique using iodine as a transport agent. As a starting material we employed a polycrystalline $CuAlS_2$ compound synthesized by direct melting of the constituent elements in a BN crucible at temperature of 1300°C.[7] The resulting undoped crystals were typically bulk-shaped with dimensions of about $6 \times 3 \times 1.5$ mm^3, the colouration of the crystals being transparent green due to the charge-transfer transitions introduced by residual transition atom (TA) impurities.[8]

2.2 *Zn-doping processes*

Zn-doping was carried out by using different techniques described below, with thermal treatments having been carried out for various durations in the range 20–120 h. The processes are as follows:

(1) Introducing Zn-impurity directly into the mixture of the constituent elements prior to the synthesis of the compound.

(2) Thermal treatments of undoped crystals in the presence of ZnS powder or metallic Zn with sulphur added into the ampoule.

(3) Annealing undoped crystals in the presence of metallic Zn with the amount of Zn (per unit volume of the ampoule) of 15 mg/cm^3 (designated as Zn_1) without sulphur at sufficiently low annealing temperatures $T_a < 600$°C.

(4) Annealing undoped crystals with a larger amount of Zn or at higher annealing temperatures (T_a>700°C). For example, crystals annealed with a Zn amount of 150 mg/cm^3 (designated as Zn_2) show a morphology different from case (3) as described in §3.3.

These different Zn-doping techniques result in different concentrations of the Zn-dopant incorporated in the host lattice. Relatively low (less than 1 mol%) Zn concentration was realized in processes (1)–(3), while heavy Zn-doping was possible in the process (4) as described in §3.1.

2.3 *Analysis of composition*

The chemical composition of as-grown crystals was determined by the inductively coupled plasma emission spectroscopy (ICP) technique for Cu, Al and Zn (in case of Zn-doped samples) and by the atomic absorption analysis (AAA) for S, the relative inaccuracy of both analyses being nearly 1%.

Polishing of the samples was carried out by using lapping films (3M Corp., 3 and 1 μm particles) with subsequent cleaning in methanol. Some of the Zn-doped crystals were subsequently annealed in vacuum or sulphur vapour. The adhering sulphur in the last case was removed by rinsing the sample in hot carbon disulfide.

The distribution of composition on the surface of a polished specimen of heavily Zn-doped crystal was measured by electron probe microanalysis (EPMA) using a Shimadzu EPMA-8700 microanalyzer with an electron acceleration voltage of 15 kV and sample current of 0.1 μA.

2.4 *Photoluminescence*

Photoluminescence (PL) was studied in the temperature range 4.2–520 K and was excited by the 325 nm line of a He–Cd laser (10 mW power, excitation intensity 0.5 W/cm^2), with the samples being put into an Oxford Instruments continuous-flow cryostat. The emitted PL was dispersed by a JASCO CT-25C monochromator with a focal length (FL) of 25 cm and 1200 groove/mm grating blazed at 750 nm, and detected by a Hamamatsu R928 photomultiplier (PM). The spectral resolution was 0.6 nm (3 meV at 500 nm).

For measurements of PL-excitation (PLE) spectra, which were carried out at 2 K, a 150 W Xe-lamp combined with an Acton Research Spectra Pro 275 monochromator with a FL of 27.5 cm was used as an excitation source. The emitted light was again dispersed by a Spex 500M monochromator with a FL of 50 cm, and detected by a Hamamatsu R943-02 PM. In both monochromators the 1200 groove/mm gratings blazed at 500 nm were used.

3. Results and Discussion

3.1 *Chemical composition of Zn-doped samples*

Compositions of samples doped with Zn by the processes (1) and (2) thus determined can be expressed by chemical formulae $Cu_{0.96}Al_{1.04}Zn_{0.001}S_{2.18}$ (hereafter denoted as $CuAlS_2$:Zn0.1 mol%) and $Cu_{0.95}Al_{1.05}Zn_{0.005}S_{2.19}$ (denoted as $CuAlS_2$:Zn0.5 mol%), respectively. The compositions were found to show a considerable deviation from stoichiometry with a ratio of Al/Cu being in the range 1.05–1.10 (the inaccuracy being ±1%) implying the presence of high concentration of Cu-vacancies or Al_{Cu} antisite defects. The Zn-concentration of samples obtained by the process (3) was less than 1 mol% and shows a considerable gradient from surface to inside. Therefore in this case we do not show analyzed concentration.

Analyzed composition of one of the heavily doped samples obtained by the process (4) was $Cu_{0.905}AlZn_{0.12}S_{2.14}$. However, this composition can be regarded as only a nominal one, since a gradient of Zn-concentration from the surface to the bulk, as well as a multiphase structure (described later in the text), was also observed.

3.2 *Reduction of green colouration in Zn-doped samples*

The green colouration in undoped crystals was completely reduced by Zn-doping. The colouration in undoped $CuAlS_2$ crystals has been attributed to the presence of Fe^{3+}-related charge-transfer absorption bands peaked at 620 and 920 nm. According to our previous studies,[8] quenching of the Fe^{3+}-related absorptions implies the upward-shift of the Fermi level in the band gap in relation to the Fe^{2+}/Fe^{3+} demarcation level, caused by an increase of the concentration of donor-like lattice defects. Therefore, the reduction of colouration in lightly Zn-doped samples implies that Zn acts as a donor-like defect. We believe Zn substitutes mainly for the Cu-sites with the formation of the donor-like Zn_{Cu}-defects.

3.3 *Crystal structures and morphologies in Zn-doped crystals*

Figure 1 shows results of the X-ray powder analysis of (a) an as-grown crystal of undoped $CuAlS_2$, (b) a crystal annealed with a small amount of Zn metal (Zn_1: 15 mg/cm^3) at 600°C, (c) a crystal annealed with a large amount of Zn metal (Zn_2: 150 mg/cm^3) at 750°C and (d) a heavily Zn-doped crystal which was obtained by annealing, with Zn_2 at 900°C.

Figure 1(b) indicates that the bulk of samples doped with Zn in low concentrations (x<0.5 mol%) remains single phase of the chalcopyrite structure, since no new reflections have been observed for slightly Zn-doped crystals as compared with the undoped $CuAlS_2$ (Fig. 1(a)).

The X-ray analysis in the heavily doped crystals (Figs. 1(c) and 1(d)) shows a quenching of chalcopyrite phase diffractions and an appearance and an increase in intensities of diffraction peaks of the spinel type cubic phase of $ZnAl_2S_4$, the $CuZn_5$ alloy and ZnS-related structures with the increase of the annealing temperature.

Although the surfaces of the samples, doped under an excess S pressure, remain smooth and clean, doping without addition of S in the ampoule results in formation of yellow-red blotches on the surface of samples due to alloying of Zn with $CuAlS_2$, this result being similar to that reported for Zn-doped $CuGaS_2$.[9] The red

blotches have been removed by etching in 1:1 HCl:HNO_3 for 1 min.

In heavily Zn-doped crystals, the above-mentioned blotches grow to cover the whole surface of the crystal with formation of a "network"-like structure on the original surface, which is shown in Fig. 2(a) for the sample annealed for 60 h at 800°C with a presence of Zn in the amount Zn_1 in the ampoule. Moreover, this structure has been found to develop into the bulk of the crystals. Optical micrograph of the structure at the depth $d=30\ \mu m$ is shown in Fig. 2(b). The structure consists visually of two regions, that is the "light" region and the "dark" one.

The composition of the light region has been identified by the EPMA technique as a metallic alloy $CuZn_5$ (85%) with an admixture of CuAl phase (15%), whereas the dark region has been identified as consisting of a spinel phase with the composition $ZnAl_2S_4$ (80%) with the admixture of the original $CuAlS_2$ chalcopyrite phase (15%), as well as of both sphalerite and wurtzite ZnS phases (5%). This result is consistent with the result of the X-ray powder diffraction analysis.

Hence, due to the alloying of Zn with $CuAlS_2$ at high enough annealing temperature T_a the original crystal lattice decomposes with the formation of several non-chalcopyrite phases. It should be pointed out that adding of S in the ampoule with the S-pressure being

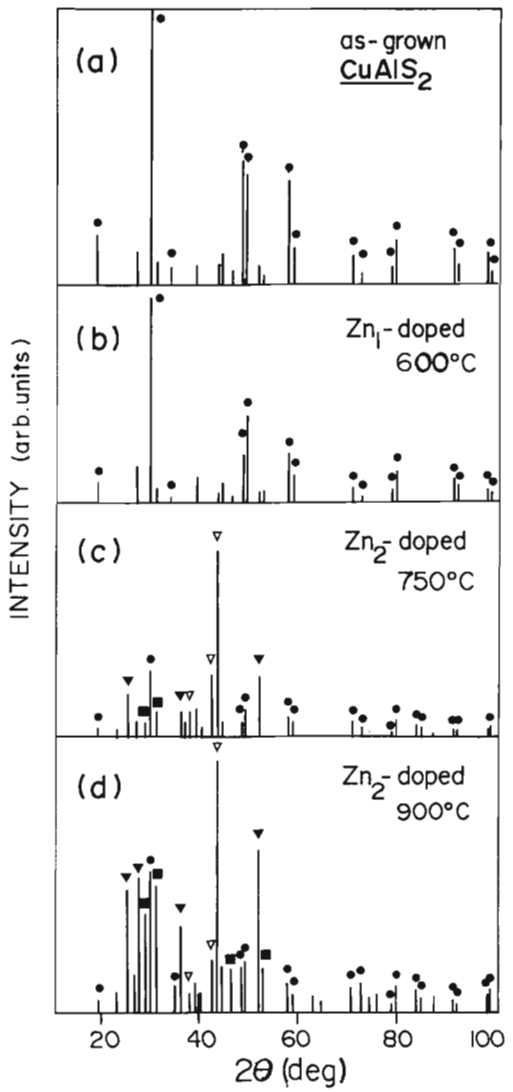

Fig. 1. X-ray powder diffraction patterns for the undoped (a) as well as Zn-doped (b–d) $CuAlS_2$, with the amount of Zn per unit volume of the ampoule being $Zn_1=15\ mg/cm^3$ (b) and $Zn_2=150\ mg/cm^3$ (c, d), and the annealing temperatures being 600°C (b), 750°C (c) and 900°C (d). The marks on the top of reflections correspond to the different phases, i.e.
●—$CuAlS_2$ chalcopyrite,
▽—CuZn alloy,
▼—$ZnAl_2S_4$ spinel,
■—ZnS cubic, hexagonal.
Unmarked reflections relate to the Cu_xS_y phases, usually observed in CVT-grown $CuAlS_2$.

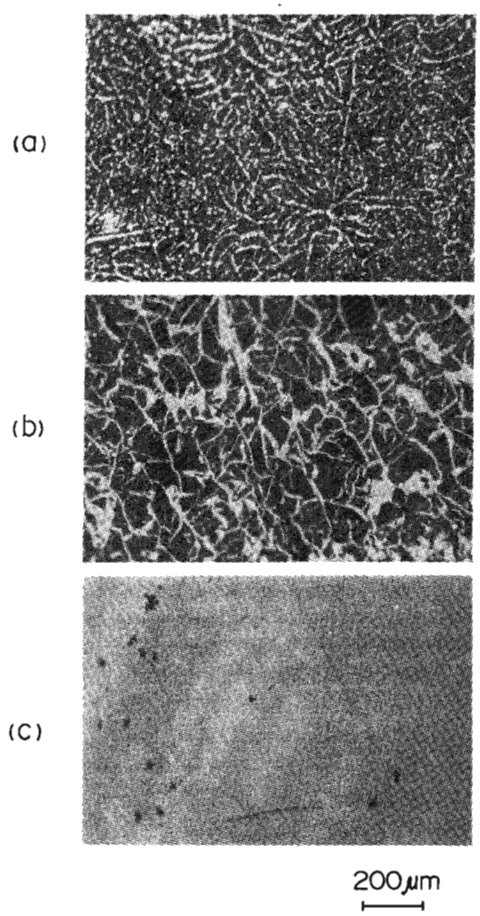

Fig. 2. Optical micrographs of the heavily Zn-doped $CuAlS_2$. (a) The structure developed on the surface after doping. (b) The structure developed in the bulk, the layer of $d=30\ \mu m$ has been removed from the surface by polishing. (c) The original $CuAlS_2$ phase found deep in the bulk, $d=200\ \mu m$.

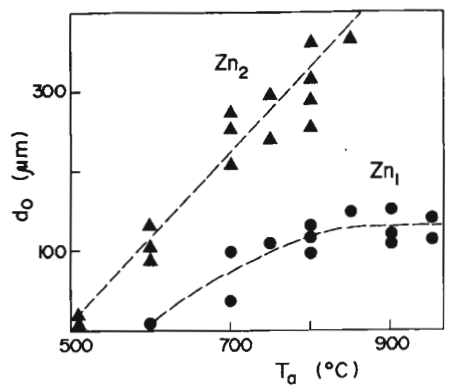

Fig. 3. Dependence of the multiphase structure proliferation depth d_0 in the bulk on the annealing temperature T_a for two amounts of Zn added into the ampoule
●—Zn_1=15 mg/cm^3,
▼—Zn_2=150 mg/cm^3.

higher than 1 atm serves to "protect" the surface of the samples—no multiphase structure has been formed in this case at any annealing temperature.

A step-by-step polishing of Zn-doped samples with the subsequent microscopic observation shows that, as we move from the original surface into the bulk of the samples, the relative amount of the metallic alloy phase decreases rapidly and, at the same time, the amount of the $ZnAl_2S_4$ and ZnS phases as compared with that of the chalcopyrite phase also decreases until, at some depth in the bulk, only original $CuAlS_2$ phase is observed (Fig. 2(c)). The dependence of the terminal depth d_0 (the distance from the original surface) of the decomposition of the chalcopyrite phase is shown in Fig. 3 as a function of the annealing temperature for two amounts of added Zn in the ampoule-Zn_1 (15 mg/cm^3) and Zn_2 (150 mg/cm^3). It can be seen that at lower amount of added Zn (Zn_1) the decomposition of the crystal surface begins at T_a~600°C, and d_0 tends to saturate at the values of d_0 in the range 110–150 μm. At higher amount of added Zn (Zn_2) d_0 increases rapidly with T_a without any sign of saturation until, at high enough T_a, the bulk of the original $CuAlS_2$ crystal entirely turns into the multiphase structure.

It has been found out that the formation of this multiphase structure serves to increase drastically (by an order 10^2–10^3) the intensities of the emission bands, observed in Zn-doped $CuAlS_2$, which is discussed in the next paragragh.

3.4 *Photoluminescence*

3.4.1 *Relatively low Zn concentration*

The PL spectra for the crystals doped with Zn by the process (1) (doping into the starting materials) described in §2.2 are shown in Figs. 4(a) and 4(b) corresponding to Zn concentration of 0.5 mol% and 2 mol% (analyzed by ICP), respectively. As shown in Fig. 4(a), the spectrum of the sample with Zn concentration of 0.5 mol% exhibits three free-to-bound (FB) emissions

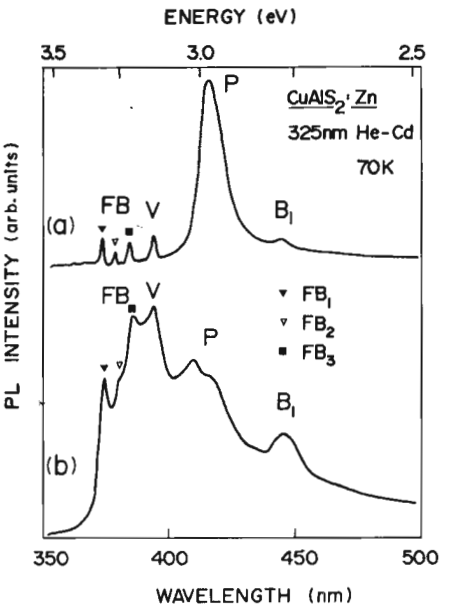

Fig. 4. PL spectra of the lightly Zn-doped $CuAlS_2$ crystals. Doping has been carried out by adding the metallic Zn into the mixture of constituent elements prior to the $CuAlS_2$ compound preparation, the concentration of Zn in the resulting crystals being (a) x=0.5 mol% and (b) x=2 mol%.

peaked at 372 nm (=3.33 eV) (▼), 378 nm (3.27 eV) (▽) and 383 nm (=3.23 eV) (■), and stronger purple emission (denoted as P) at 415 nm (2.99 eV), which are usually observed in the undoped $CuAlS_2$,[1-3] as well as two weak emissions peaked at 393 nm (3.15 eV) and 445 nm (2.79 eV) (designated as V and B_1, respectively) which have not been observed in the undoped crystals. As illustrated in Fig. 4(b), increase of Zn concentration up to 2 mol% serves to increase the intensities of the FB and Zn-related V- and B_1-emissions. The samples obtained by process (2) (annealed in ZnS or metallic Zn plus excess S-pressure) exhibit essentially the same spectra as shown in Fig. 4, with either V- or P-emission being dominant. Sometimes broad weak emissions peaked at 480 nm (2.58 eV) and 520 nm (2.38 eV) could also be detected in these lightly Zn-doped crystals.

In the spectra of the crystals obtained by the process (3) (annealed in Zn without addition of S in the ampoule), the V-emission is greatly enhanced as compared with the above discussed cases, and turns to dominate the spectrum at low temperatures, with weak FB- and B_1-emissions being sometimes also observed.

On the basis of time-resolved PL measurements the V-emission has been tentatively attributed to a donor-acceptor pair recombination involving a native acceptor (V_{Cu}) with activation energy 0.18 eV and a Zn-introduced donor-like Zn_{Cu} defect with activation energy 0.32 eV.[10]

Figure 5 shows V-emission of the samples annealed

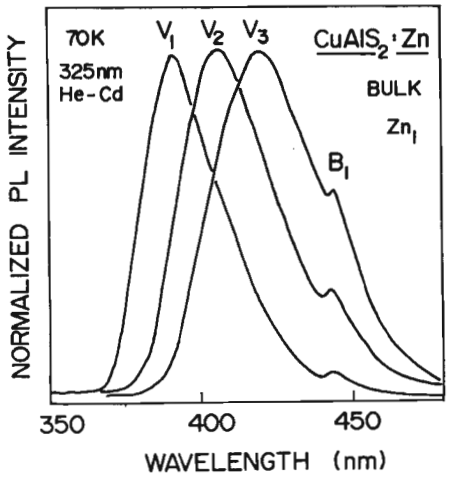

Fig. 5. Dependence of the peak position V_p of the V-emission on the annealing temperature T_a.
V_1 T_a=700°C V_p=390 nm
V_2 T_a=800°C V_p=405 nm
V_3 T_a=950°C V_p=425 nm.
The samples were annealed in Zn in the amount Zn_1 and polished to the depth d=150 μm to remove the multiphase structure.

in the presence of Zn in the amount Zn_1 at annealing temperatures T_a=700°C, 800°C and 950°C. Prior to the PL measurements the samples were etched in 1:1 HCl:HNO_3 and polished to the same depth d=150 μm to remove the multiphase structure formed in the presurface region. The peak position of the V-emission shows a shift toward low energies with an increase of the annealing temperature. We believe the peak position undergoes a real shift, not redistribution of intensities between several emissions from different centers, because (1) the peak position of the V-emission shifts with T_a continuously, (2) shoulders, superposed on the V-emission, which may indicate the presence of several emission subcomponents, have never been observed in our spectra. We tentatively attribute the observed shift of the V-emission with T_a to increased broadening of the energy level, introduced into the band gap of $CuAlS_2$ by the Zn_{Cu}-defects, with rising of T_a due to the increase of Zn concentration in the samples. The similar large low-energy shift of the PL bands with the increase of the Zn concentration in the samples has been observed for Zn-doped $CuGaS_2$.[9,11]

3.4.2 *High Zn concentration*

We have already discussed the decomposition of the $CuAlS_2$ compound with the formation of the multiphase structure on the surface and in the bulk for the heavily Zn-doped samples, annealed in the presence of Zn in the concentration Zn_1 (Zn_1-doped) at T_a>600°C or Zn_2 (Zn_2-doped) at T_a>500°C (Fig. 3). It turns out that this multiphase structure formation gives rise to the extremely bright blue and green emissions, the dominant emission being determined by the Zn-doping conditions. In all heavily doped samples under investigation the surfaces have been found to emit bright green PL even at RT, whereas the bulk emits either the V-emission for Zn_1-doped samples with d>150 μm (original $CuAlS_2$ phase) or a blue emission for the Zn_2-doped samples with d=100–300 μm (the multiphase structure still being observed).

The dependence of the PL spectra on the distance from the original surface for the Zn_1-doped sample, annealed at T_a=700°C, is shown in Fig. 6. The surface of the sample emits three PL bands, i.e. the previously discussed V- and B_1-emissions, as well as a broad green G-emission peaked at 510–525 nm. A step-by-step polishing of the sample leads to the rapid quenching of the G-emission and serves to shift the V-emission peak from 425 to 390 nm.

The shift of the V-emission can be explained by the decrease in the concentration of Zn-introduced ZnCu defects as we move from the surface of the sample in the bulk, these results being in accordance with those shown in Fig. 5.

The increase of the Zn amount in the ampoule from Zn_1 (15 mg/cm^3) to Zn_2 (150 mg/cm^3) results in the appearance of the blue emission peaked at 480 nm (=2.58 eV) (labeled as B_2), discernible in the PL spectrum from the surface at low temperatures, which is shown in Fig. 7. It can also be seen that the dominant G-emission is still clearly observable even at the temperature as high as 500 K (the upper temperature limit of our cryostat), when all other emissions are already thermally quenched.

Polishing of this sample to the depth d=200 μm (some traces of the multiphase structure still being observed) serves to diminish greatly the G-emission intensity with the B_2-emission turning to dominate the spectrum at low temperatures. However, at temperatures higher than 50°C (320 K) the G-emission turns to dominate the spectrum again due to the "negative" thermal quenching of the G-emission, which will be dis-

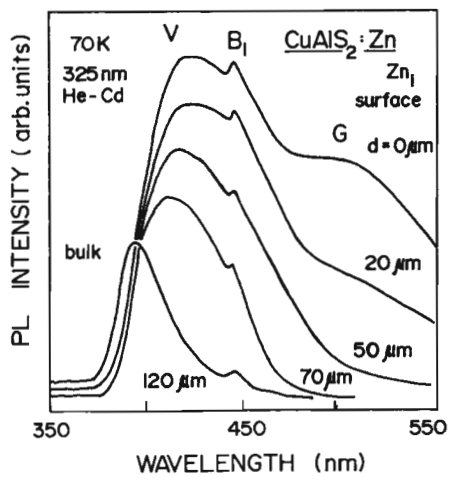

Fig. 6. Dependence of the V-, B_1- and G-emissions on the distance from the surface for the Zn_1-annealed sample (T_a=700°C). The thickness of the layer, polished off prior to the PL measurements, is indicated on the right side of the corresponding curves.

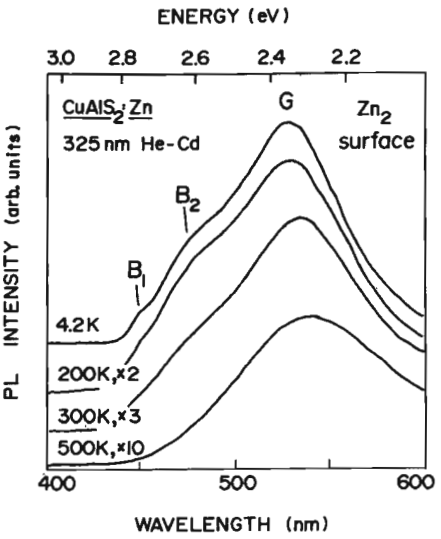

Fig. 7. PL spectra of the Zn_2-doped sample (T_s=800°C), taken from the surface ($d<20\ \mu m$), for various temperatures.

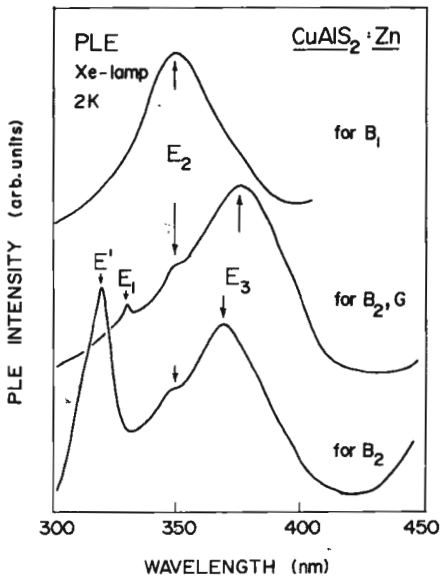

Fig. 8. PLE spectra for the B_1-emission (upper curve), and B_2- and G-emissions (middle curve). At some points of the sample an excitation peak E′ has also been observed (lower curve) for the B_2-emission.

cussed later.

We believe that the above-mentioned visible emissions except for the B_2-line can be associated with the $CuAlS_2$ phase in the multiphase structure, since these emissions have been observed, though of weak intensity, also in lightly-doped crystals in which no phase separation occurs. We also assume the B_2 is caused by a transition in the $CuAlS_2$ phase taking into account the PLE spectra and the temperature dependence of its intensity, which will be discussed in §3.5 and §3.6, respectively.

3.5 *Photoluminescence excitation spectrum (PLE) in heaviy doped samples*

PLE spectra were measured only in heavily Zn-doped crystals, since emissions of lightly Zn-doped crystals were too weak to give a reliable PLE spectrum with an excitation by the monochromatic light from a Xenon-light source dispersed by the monochromator. PLE spectra for the visible emissions measured in a heavily Zn-doped crystal are shown in Fig. 8. The PLE spectrum for the B_1-emission, this emission having been observed also in lightly-doped crystals, exhibits one maximum E_2, the spectral position of which (350 nm, 3.54 eV) corresponds to the band gap energy of $CuAlS_2$. Therefore, the B_1-emission is believed to be excited by direct band-to-band electronic transitions and can safely be assigned to emissions related to some defects in $CuAlS_2$.

The G-emission and, in most cases, also the B_2-emission exhibit a similar and quite complicated PLE spectrum, shown in the middle of Fig. 8. The fact that the emissions B_2 and G share the same PLE spectrum leads us to conclude that the B_2-emission is related to the same center as the G-emission. Since the G-emission has been observed in the lightly-doped crystals in which no phase separation occurs, we can assume that the both emissions are related to a common defect (or impurity) center in $CuAlS_2$.

The PLE spectrum consists of three features, i.e., a sharp peak E_1 at 334 nm (=3.71 eV), a shoulder E_2 at 350 nm (=3.54 eV), as well as a broad band E_3, the peak position of which has been found to change in the range 370–385 nm depending on samples. The E_1-peak can be attributed to electronic transitions from the lower subband (Γ_6-symmetry) of the valence band into the conduction band since the spectral position of the E_1-peak (3.71 eV) corresponds to the energy separation between the Γ_6-valence subband and the conduction band.[12] The E_2-shoulder represents, obviously, the same transitions from the upper valence subband of Γ_7-symmetry into the conduction band as were observed for the B_1-emission (upper curve). The E_3-peak at 370–385 nm (3.35–3.22 eV) may be assigned to the band-tail absorption caused by large concentration of the crystal defects since native defects introduce several relatively shallow energy levels with E_a=200–300 meV in the band gap of $CuAlS_2$, which follows from the observation of the several free-to-bound transitions, discussed in Introduction. Since the concentration and species of native defects involved are supposed to be dependent on samples, the position of the E_3-peak changes from one sample to another.

Therefore, the B_1- and G-emissions are believed to be excited by the absorption in the $CuAlS_2$ host compound.

However, at some points of the sample a high-energy

E′-peak has also been observed in the PLE spectra of the B_2-emission (Fig. 8, the lowest curve). Since the spectral position of the E′-peak (320 nm, 3.87 eV) is higher than any band edge transition energies in the $CuAlS_2$, this peak may be tentatively attributed either to the direct excitation of the excited states in some Zn-introduced defect center, taking part in the B_2-emission, or to the absorption in one of the nonchalcopyrite phases of the multiphase structure, the latter assumption being quite plausible as will be discussed in §3.7.

3.6 *Temperature dependence of the PL intensities in heavily Zn-doped samples*

As mentioned above, we have assumed that all the visible emissions are originated from radiative transitions between gap-states in $CuAlS_2$ phase. In order to determine the energy positions of these gap states involved in the transitions, we measured temperature dependences of the PL intensities of individual emissions, which are often referred to as thermal quenching curves, the results being plotted in Fig. 9.

Temperature dependence of the G-emission (upper curve) exhibits two remarkable features, such as (1) an increase of intensity at temperatures ranging between 280 and 340 K with a "negative" thermal activation energy $E_{aT}^{-}\sim 170$ meV, and (2) a very rapid thermal quenching at higher temperatures, from which activation energy of the defect, involved in this emission, has been deduced as $E_{aT}=700\pm30$ meV. Temperature dependence of the B_2-emission (middle curve) also exhibits some increase in intensity at temperatures from 200 to 300 K (although not as remarkable as for the G-emission), and thermal quenching with an activation energy $E_{aT}=610\pm40$ meV. Here, we have witnessed a similarity in temperature dependences between the G- and the B_2-emissions.

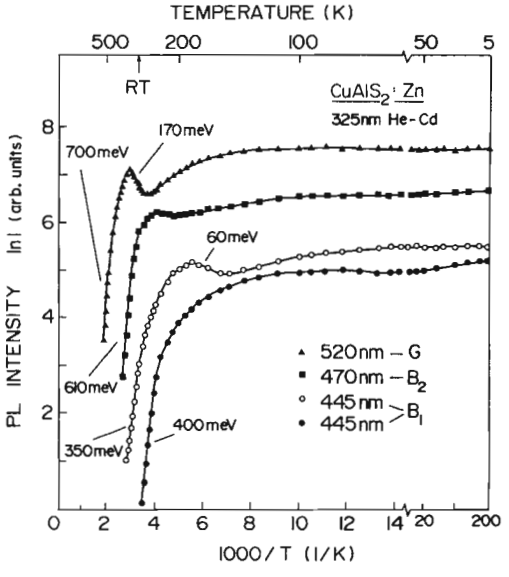

Fig. 9. Temperature dependencies of the intensities of the visible emissions.

The luminescence quenching of the B_1-emission was found to depend on the sample (two lower curves). For one of the investigated samples the emission intensity increases in the temperature range 150–200 K with E_{aT}^{-} 60 meV and subsequent thermal quenching with $E_{aT}=350\pm30$ meV, whereas for two other samples no "negative" quenching has been observed, the emission intensity being decreased with $E_{aT}=400\pm30$ meV. Although at RT the B_1-emission intensity is only of the order of 5% as compared with that for the G-emission, the B_1-emission is still quite strong and is visually observable up to 120°C.

The observed increase, in some temperature range, of the intensities of emissions with increasing temperature, which was called "negative thermal quenching", has also been observed for the blue emission in ZnS.[14] It is assumed that this "negative" thermal quenching of emissions occurs due to the thermal depopulation between, at least, two defect levels, with the "negative" activation energy being equivalent to the energy difference between these two levels. This effect is believed to be responsible for the high intensity of the visible emission even at temperatures higher than RT.

Taking into account that the energy separation between the spectral position of the free exciton emission (3.55 eV at 10 K) of undoped $CuAlS_2$ and the peak positions of the B_1-, B_2- and G-emissions is found to be much larger than the corresponding activation energies for these emissions deduced from the thermal quenching curves (Fig. 9), the observed visible emissions may tentatively be attributed to the donor-acceptor pair recombination involving deep Zn-introduced defects. The large values of half-width of the visible emissions is an indication of a strong phonon or resonant-localized-modes coupling, which would be expected for deep centers.

3.7 *Multiphase structure and photoluminescence*

As mentioned before, we believe that all the visible emissions observed in the heavily-doped samples originate from the $CuAlS_2$ compound. The remarkable result of the present study is that they are found to be greatly strengthened in heavily doped samples, when the multiphase structure is formed. The mechanism responsible for the observed strengthening of the visible emissions still remains unclear. Our tentative explanation is that electron and holes produced by the photoexcitation (with PLE peak of E′) in unidentified wide gap phase are efficiently transferred to lower energy $CuAlS_2$ phase through the heterojunction formed at the phase boundary and lead to the B_2-emission by radiative recombination process. The spinel $ZnAl_2S_4$ compound found by X-ray analysis and confirmed by EPMA is a highly plausible candidate for such a wide gap phase since the material is expected to have the band gap energy of 4.0 eV,[13] which is close to the spectral position of the E′-peak. Crystal growth and optical studies in the $ZnAl_2S_4$ compound would be of interest and are planned for the future studies.

Furthermore, since Zn may well be expected to sub-

stitute for both Cu and Al sites in the $CuAlS_2$ crystal lattice, forming both the donor-like and the acceptor-like defects and, moreover, since complexes consisting of one or more Zn atoms and various native defects may also be formed, it is impossible at a present stage to ascertain definitely the nature of the centers, responsible for the blue and green emissions.

It can only be noted that annealing of the Zn-doped samples in vacuum serves to quench the V-emission, and to strengthen greatly the G-emission independently of previous treatments of the samples. These results, as well as the above discussed "protection" of the surface of samples by S-vapour, show an importance of S-vacancies in the formation of multiphase structures and strengthening of the visible emissions.

4. Conclusions

In conclusion, the experimental results obtained in this study show that $CuAlS_2$ crystals, lightly doped with Zn, emit violet emission peaked at 390 nm. In heavily Zn-doped samples, decomposition of original surface and presurface region of samples with formation of multiphase structure has been observed. The formation of the multiphase structure was dependent on the Zn-doping conditions. This structure has been found to emit very bright blue emissions peaked at 445 and 480 nm, as well as the green emission peaked at 520 nm, these emissions exhibiting remarkable features, such as "negative" thermal quenching due to the thermally induced redistribution of carriers between several defect states, this effect, in its turn, being responsible for maintaining the intensities of the emission at high level even at high temperatures. The results obtained suggest that the $CuAlS_2$ compound may be considered as a perspective material for the blue and green light emitting device realization.

Acknowledgments

We would like to thank Dr. Takashi Yasuda of RIKEN for PLE measurements and fruitful discussions. We also express our appreciation of the support on this study by the Japan Society for the Promotion of Science and by a Grant-in-Aid for Scientific Research from the Ministry of Education, Science and Culture.

1) S. Shirakata, I. Aksenov, K. Sato and S. Isomura: Jpn. J. Appl. Phys. **31** (1992) L1071.
2) I. Aksenov, I. Gulakov, V. Lipnitskii, A. Lukomskii and L. Makovetskaya: Phys. Status Solidi a **115** (1989) K113.
3) N. Yamamoto: *Proc. 4th Int. Conf. Ternary and Multinary Compounds, Tokyo, 1980*, Jpn. J. Appl. Phys. **19** (1980) Suppl. 3, p. 95.
4) Y. Kudo, N. Kojima, Y. Takada, I. Aksenov and K. Sato: Jpn. J. Appl. Phys. **31** (1992) L663.
5) I. Aksenov and K. Sato: Appl. Phys. Lett. **61** (1992) 1063.
6) I. Aksenov and K. Sato: *Rec. 11th Symp. Alloy Semiconductor Physics and Electronics, Kyoto, 1992* (Alloy Semiconductor Physics and Electronics Secretariat, Kyoto, 1992) p. 67.
7) I. Aksenov, Y. Kudo and K. Sato: Jpn. J. Appl. Phys. **31** (1992) L145.
8) I. Aksenov and K. Sato: Jpn. J. Appl. Phys. **31** (1992) 2352.
9) J. L. Shay, P. M. Bridenbaugh and H. M. Kasper: J. Appl. Phys. **45** (1974) 4491.
10) I. Aksenov, T. Yasuda, Y. Segawa and K. Sato: to be published in J. Appl. Phys.
11) A. Ooe and S. Iida: Jpn. J. Appl. Phys. **29** (1990) 1484.
12) N. Syrbu, N. Rabotinskii, G. Stratan and S. Khachaturova: Sov. Phys. Solid State **30** (1988) 1655.
13) O. Kulikova, L. Kulyuk, N. Moldovian, S. Popov, D. Remengo and A. Siminel: *Proc. 8th Int. Conf. Ternary and Multinary Compounds, Kishinev, 1990* (Moldavian Academy of Sciences, Kishinev, 1990) p. 353.
14) T Yokogawa, T. Taguchi, S. Fujita and M. Satoh: IEEE Trans. Electron Devices **ED30** (1983) 271.